IEEE Photonics Journal
An IEEE Photonics Society Publication

Open Access

A Symmetrical Dual-Beam Bowtie Antenna With Gain Enhancement Using Metamaterial for 5G MIMO Applications

Volume 11, Number 1, February 2019

Haixin Jiang
Li-Ming Si
Weidong Hu
Xin Lv

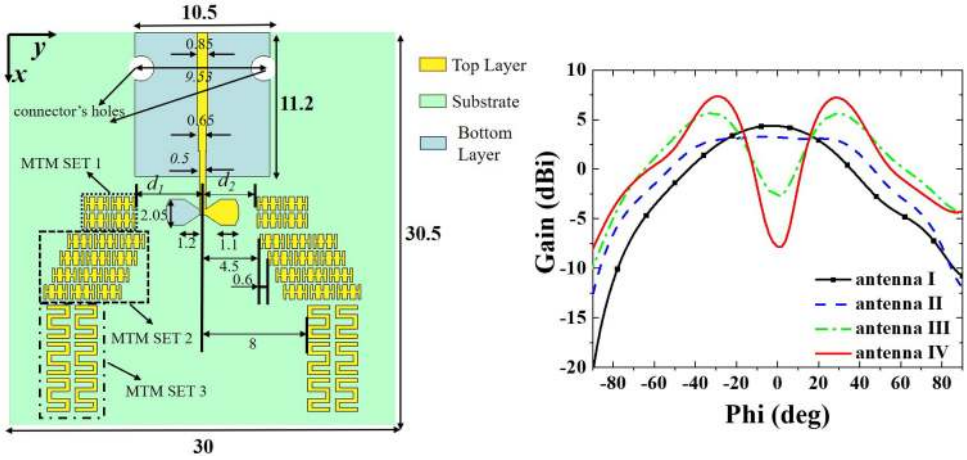

DOI: 10.1109/JPHOT.2019.2891003
1943-0655 © 2019 IEEE

A Symmetrical Dual-Beam Bowtie Antenna With Gain Enhancement Using Metamaterial for 5G MIMO Applications

Haixin Jiang, Li-Ming Si, Weidong Hu, and Xin Lv

Beijing Key Laboratory of Millimeter Wave and Terahertz Technology, School of Information and Electronics, Beijing Institute of Technology, Beijing 100081, China

DOI:10.1109/JPHOT.2019.2891003

Manuscript received December 13, 2018; revised December 28, 2018; accepted December 31, 2018. Date of publication January 4, 2019; date of current version January 18, 2019. This work was supported in part by the National Key R&D Program of China under Grant 2018-YFF0212103, in part by the National Natural Science Foundation of China under Grant 61527805, in part by the Higher Education Discipline Innovation Project of China (111 project) under Grant B14010, in part by Shanghai Pujiang Program under Grant 18PJ1403200, and in part by the Research Base Foundation of Beijing Institute of Technology under Grant 3050012211803. Corresponding author: Li-Ming Si (e-mail: lms@bit.edu.cn).

Abstract: A symmetrical dual-beam end-fire bowtie antenna with gain enhancement is achieved by integrating three pairs of metamaterial (MTM) arrays for 5G MIMO applications. The first pair of MTM array with high refractive index (HRI) are deployed to form a wide beam antenna. The second pair of HRI MTM array are arranged along the end-fire direction (*x*-direction) in front of the radiators in order to split the single wide beam into dual beam. Besides, the third pair of anisotropic MTM array with HRI along *x*-direction and near zero refractive along *y*-direction are incorporated in front of the second pair of MTM array to improve the gain performance. The proposed technique is verified by both the full-wave electromagnetic simulation and experiment, and the simulated and measured results agree very well with each other. Moreover, the measured results reveal that the main beam directions of the proposed antenna point to $\pm 30^{\circ}$ with respect to the end-fire direction (0°) over 24.25–27.5 GHz, with a maximum gain of 7.4 dBi at 26 GHz and a 4.2 dB gain improvement compared to the wide beam antenna.

Index Terms: Metamaterial, zero index metamaterial, dual beam, high refractive index, 5G MIMO communications.

1. Introduction

The 5G millimeter wave frequency range bands such as 24.25–27.5 GHz and 57–64 GHz have attracted considerable attention because of their wideband characteristic, which can increase the capacity and data rate of the wireless communication systems [1]–[4]. However, working at these frequency bands suffer many challenges: 1) high path loss; 2) multipath fading effect; 3) interference effect from different channels. The high path loss can be compensated by high gain antenna [5]. Dual-beam or multi-beam antennas or arrays are required to overcome multipath fading effect and interference effect [6], [7].

A traditional method to generate dual-beam or multi-beam is to employ phased array antennas [8], which can control the beam angle effectively. However, the requirements of multiple antenna elements and the phase shifter for each antenna of this method make the structure usually complex

and the total size typically large. To simplify the structure, a dual-beam MIMO (Multi-input-multi-output) antenna without phase feed configuration has been proposed in [9]. Other approaches to produce dual-beam include employing the leaky-wave antennas and the U-slot antennas [10]–[12]. With the proper design of the leaky-wave antenna, two modes can be excited simultaneously to generate dual-beam [11], however, the dual-beam radiation pattern is varied with frequency, which restricts its application. U-slot patch antenna [12] can excite higher order TM_{02} mode, which can broaden the bandwidth of the dual-beam antenna, however, the gain difference between two beams could be around 2 dB, which leads to an asymmetrical radiation pattern.

In recent years, a number of methods based on metamaterial (MTM) have been intensively investigated to enhance the performence of antenna, such as gain enhancement [13]–[19], multi-band realization [20], [21], and tilt or steer beams [22]–[28]. The anisotropic zero-index metamaterials (ZIM) with only near zero permittivity or permeability could have better impedance matching in contrast to the isotropic ZIM, resulting in the gain enhancement [13], [14]. In [25], a dual-beam is realized at $\pm 30^\circ$ by using artifical mu-near-zero medium with an asymmetric radiation pattern and a small radiation null in the end-fire direction. An anisotropic epsilon near zero (ENZ) material is loaded vertically over the slot antenna to produce dual-beam in [26].

In this work, an inexpensive technique is proposed to realize a symmetric dual-beam planar bowtie antenna in the E-plane with gain enhancement for 5G application over 24.25–27.5 GHz. The proposed dual-beam antenna is obtained by incorporated three pairs of MTM arrays around an original bowtie antenna. Firstly, a pair of MTM arrays composed of the modified I-type unit cells with equivalent HRI are placed side by side to the radiators of the bowtie antenna to form a wide beam antenna. Then, another pair of the same modified I-type MTM arrays are incorporated in front of the radiators along the end-fire direction (x-direction) to generate the dual beam. Moreover, a third pair of MTM arrays consisting of anisotropic meander line unit cells with HRI along x-direction and near zero refractive index along y-direction are deployed in front of the second pair of MTM arrays to further enhance the directivity. A prototype of the proposed antenna is fabricated and characterized. The measured results show that a symmetric dual-beam can be realized at $\pm 30^\circ$ with respect to the end-fire direction (0°) over 24.25–27.5 GHz with a maximum gain of 7.4 dBi (-30°) and 7.3 dBi (30°) at 26 GHz. Besides, the measured reflection coefficient of the proposed dual-beam antenna is better than -15 dB over 24.25–27.5 GHz. Compared with the wide beam antenna, the gain of the proposed antenna is enhanced by 4.2 dB. Furthermore, the radiation null at end-fire direction reaches -17.6 dB at 26 GHz.

2. Mechanism of Dual Beam

The beam-tilting phenomenon could occur by means of placing the HRI medium in front of an antenna. The tilt angle of the beam is determined by the refractive index of the loaded medium [22]. Thus, dual-beam can be generated by properly deploying two sets of artificial mu-near-zero medium in front of an end-fire antenna [25].

The equivalent HRI medium area can be realized by the periodically patterned metal (i.e., metamaterial) on the substrate. Fig. 1(a) shows a MTM unit cell composed of the triple-I type metallic pattern on the Rogers5880 substrate with a permittivity constant of 2.2 and a thickness of 0.508 mm. As one of the simple structures to realize the HRI, the I-type unit cell in [29] can be regarded as an electric resonator, which can be applied to realize higher effective permittivity constant by cascading several I-type unit cells. According to the refractive index formula $n = \sqrt{\mu\epsilon}$, a higher permittivity or permeability constant will result in a higher refractive index. Fig. 1(b) displays the real part of the equivalent refractive indexes for the original substrate, the single-I type, the dual-I type, and the triple-I type MTM unit cells.

By using commercial high frequency structure simulator (HFSS), the effective medium parameters are extracted by assigning perfect electric conducting boundaries in the up and down sides of triple-I unit cell in y-direction, perfect magnetic conducting boundaries with a distance of 1 mm from the top and bottom sides of triple-I unit cell in z-direction, and two ports along the x-direction [30]. It can be observed that the equivalent refractive index can be increased obviously by loading the I-type

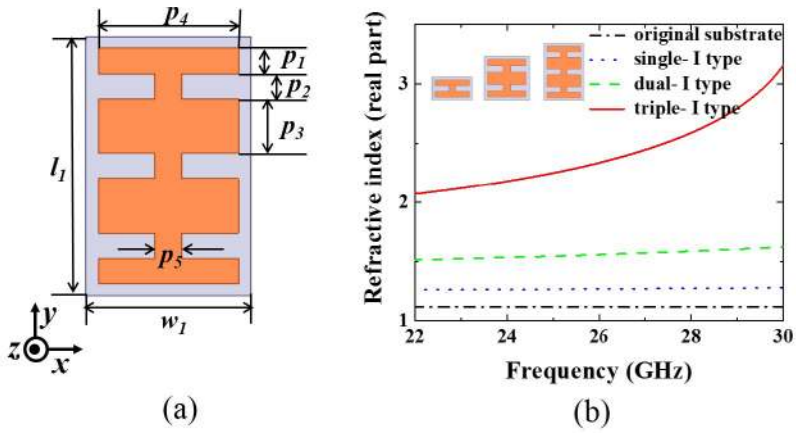

Fig. 1. (a) the structure of triple-I type unit cell (b) the comparison of real part refractive index of different number of I-type unit cell and original substrate.

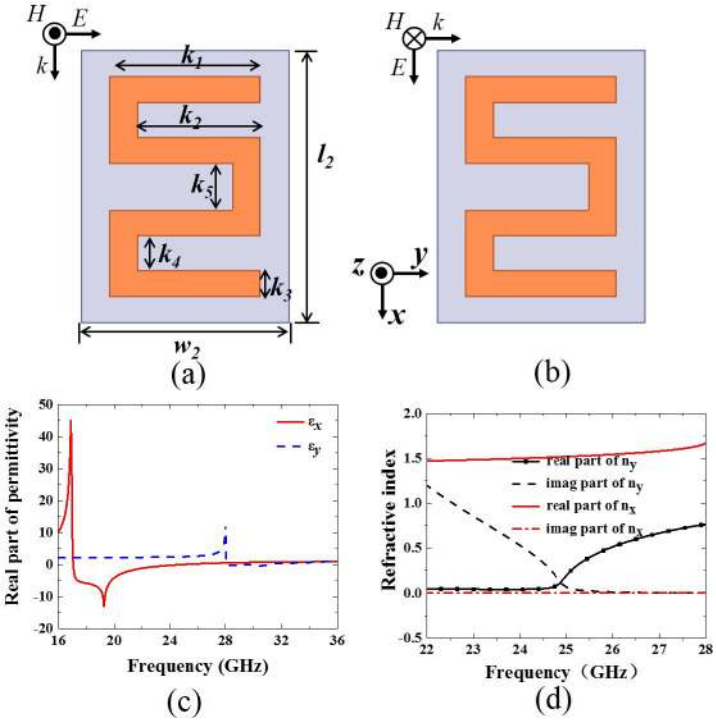

Fig. 2. Design meander unit cell structure with the incident wave propagates along (a) x-direction; (b) y-direction; (c) real part of retrieved permittivities; (d) retrieved refractive index of n_x and n_y.

unit cell on the substrate, and a higher value can be acquired by cascading more number of I-type unit cell. As expected, the triple-I type structure possesses the highest refractive index compared to the other three cases. The detailed parameters of the proposed triple-I type unit cell are set as: $p_1 = 0.2$ mm, $p_2 = 0.2$ mm, $p_3 = 0.3$ mm, $p_4 = 1.11$ mm, $p_5 = 0.2$ mm, $l_1 = 2.04$ mm, and $w_1 = 1.31$ mm. The equivalent refractive index of the triple-I type structure varies from 2.19 to 2.5 over the operating frequency range from 24.25 to 27.5 GHz, which is much larger than the refractive index of 1.12 of the original substrate. Therefore, integrating two sets of the proposed triple-I type

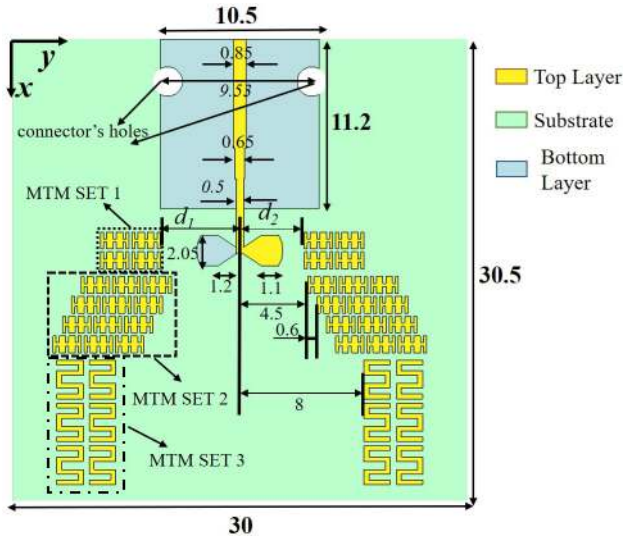

Fig. 3. The structure of the proposed antenna.

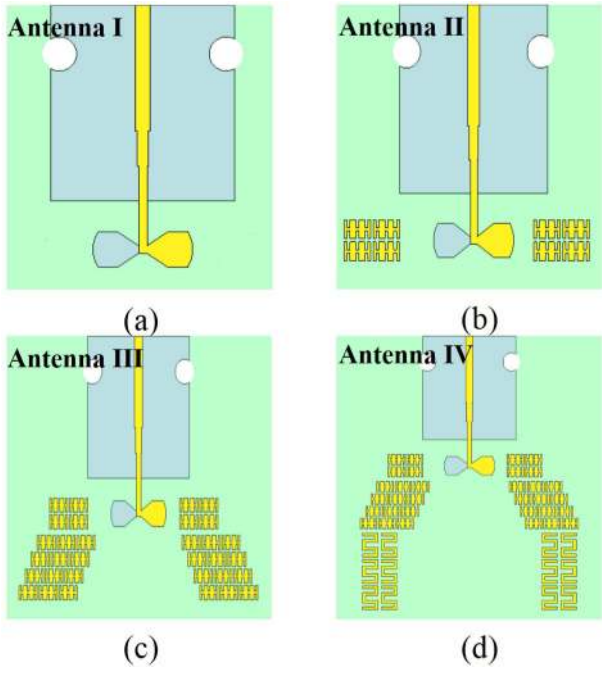

Fig. 4. The structure of four different antennas.

MTM arrays in front of bowtie antenna along end-fire radiation can alter the direction of radiation to form the dual-beam.

In addition, a meander line MTM unit cell is chosen to design an anisotropic ZIM as illustrated in Fig. 2(a) and (b) with different incident directions. The detailed parameters for the meander line are chosen as $k_1 = 1.74$ mm, $k_2 = 1.42$ mm, $k_3 = 0.3$ mm, $k_4 = 0.4$ mm, $k_5 = 0.54$ mm, $l_2 = 3.15$ mm, and $w_2 = 2.4$ mm. The metallic pattern is printed on the Rogers5880 substrate with a thickness of 0.508 mm. The electromagnetic wave propagates in x-direction with the electrical field along y-direction is illustrated in Fig. 2(a), resulting in non-resonant MTM with an almost constant ϵ_y of 2.2

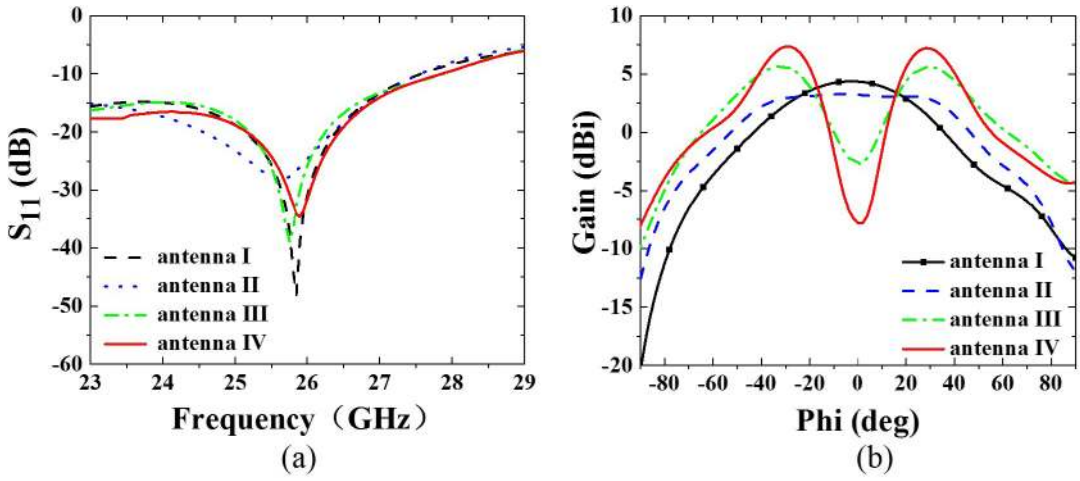

Fig. 5. (a) The S-parameters of antenna with different arrangements; (b) Radiation patterns of antenna in the E-plane with different arrangements at 26 GHz.

in the working frequency band as shown in Fig. 2(c). While the electromagnetic wave propagates in y-direction and electric field along x-direction as illustrated in Fig. 2(b), the resonance phenomenon occurs at 19.3 GHz as shown in Fig. 2(c) with near zero ϵ_x in the working frequency band over 24.25–27.5 GHz. The effective refractive indexes for these two cases are plotted in Fig. 2(d), which clearly demonstrates that the n_x and n_y are quite different. The real part of n_y is less than 0.7 and the imaginary part of n_y approaches zero over 24.25–27.5 GHz, which can be regarded as the ENZ material. In addition, n_x is varies from 1.5 to 1.6 over the frequency range of 24.25–27.5 GHz, which can be deemed as high refractive index. Hence, this anisotropic MTM can be loaded in front of the planar antenna to improve the gain.

3. Simulations and Measurements of the Dual-Beam Antenna

Fig. 3 displays the whole proposed antenna structure, which is composed of a bowtie antenna and three paris of MTM structures (labeled as MTM SET 1–3) for generating the dual-beam and improving the gain. The tapered feed line is adopted for a better impedance matching. Two holes are cut through the substrate for connecting the end launch connector from the Southeast Microwave Company [31].

In order to investigate the beam-splitting and gain improvement of the proposed MTM unit cells, four antennas illustrated in Fig. 4 are studied and compared. Fig. 4(a) shows a traditional bowtie antenna (i.e., Antenna I). Antenna II displayed in Fig. 4(b) is formed by adding a pair of 2×2 triple-I type unit cell arrays (i.e., MTM SET 1) along the y-direction of the radiator to Antenna I, which is deployed to broaden the beamwidth. In addition, Antenna III illustrated in Fig. 4(c) is constructed by integrating another pair of 4×3 triple-I type unit cells (i.e., MTM SET 2) in the end-fire direction (x-direction) of the bowtie radiators to antenna II, which is used to split the beam. Two adjacent row units have a deviation distance of 0.6 mm along y-direction as shown in Fig. 3. Finally, the proposed antenna (i.e., antenna IV) is realized by placing two sets of 3×2 anisotropic meander line structures (i.e., MTM SET 3) in front of antenna III, which aims to further increase the gain and reduce the radiation null in the end-fire direction. The parameters of the antenna and the arrangement of the three pairs of MTM arrays are detailed in Fig. 3.

The simulated S_{11} and the radiation patterns at 26 GHz of the four antennas in Fig. 4 are plotted in Fig. 5(a) and Fig. 5(b), respectively. It is observed in Fig. 5(a) that good matching ($S_{11} < -15$ dB) can be obtained over 24.25–27.5 GHz for all four antennas, which means that the matching conditions are not affected after loading the MTM structures. For Antenna I, the maximum gain in the E-plane

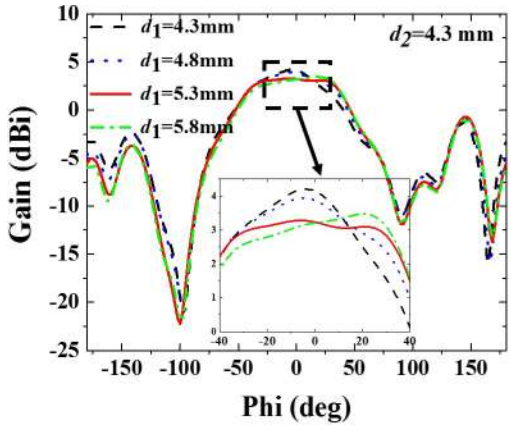

Fig. 6. Radiation patterns of proposed antenna in the E-plane with different values of d_1 at 26 GHz.

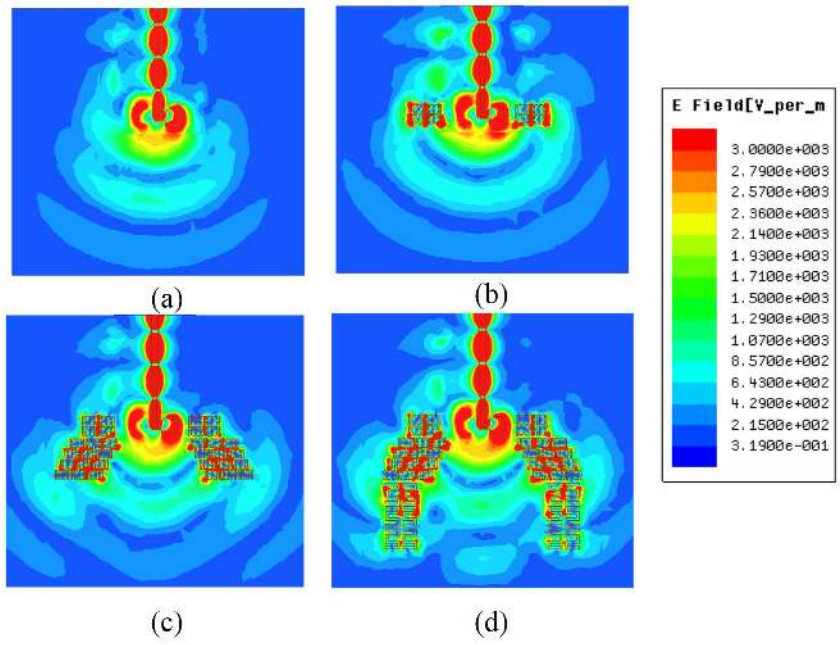

Fig. 7. The electric field distribution of antenna IV in xoy plane at 26 GHz.

at 26 GHz is 4.5 dBi with a 3 dB beamwidth of 65.4° as shown in Fig. 5(b). Compared with Antenna I, the 3 dB beamwidth of antenna II is increased by 33.2° from 63.4° to 96.6° due to the MTM SET 1, which is desirable for wireless communications, because a wider beanwith can provide a broader coverage. As mentioned in previous section, the dual-beam can be generated by placing a pair of HRI medium in front of the radiators. It is noticed in Fig. 5(b) that dual-beam phenomenon can be obtained by integrating the MTM SET 2 for Antenna III and Antenna IV. It is observed that a maximum peak gain of 5.8 dBi for Antenna III can be realized at around ±30° with respect to the end-fire direction (0°). Compared with Antenna III, due to the MTM SET 3, antenna IV shows a gain improvement of 1.7 dB and a radiation null reduction of 6.9 dB in the end-fire direction.

Furthermore, it is desirable to obtain a symmetric radiation pattern. Thus, the influence of different values of d_1 on the E-plane radiation pattern of antenna II is parametrically investigated and the

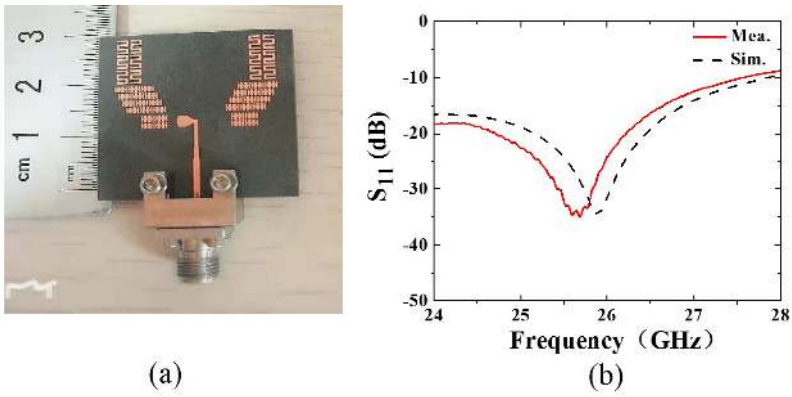

Fig. 8. (a) The fabricated antenna; (b) The simulated and measured reflection coefficient results.

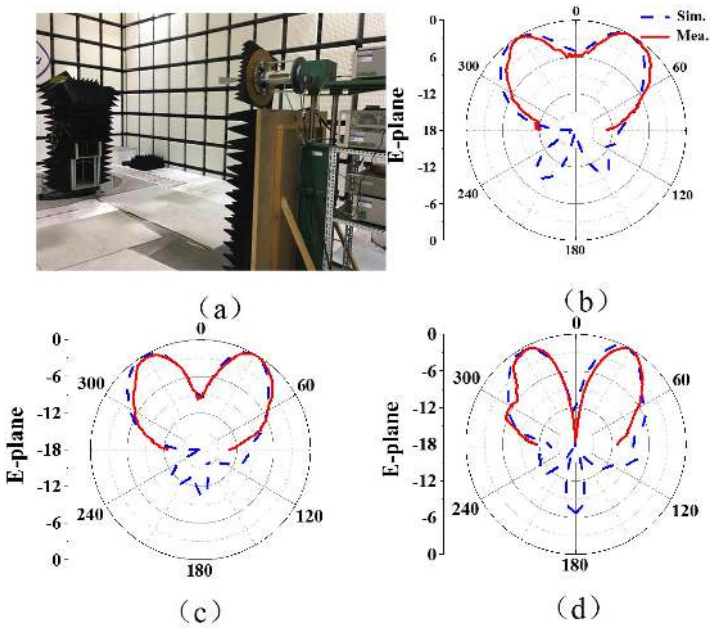

Fig. 9. (a) The setup in the anechoic chamber for measuring the radiation patterns and gain of the proposed antenna; normalized radiation patterns of the dual-beam bow-tie antenna in the E-plane at (b) 25 GHz, (c) 26 GHz, and (d) 27 GHz.

results are illustrated in Fig. 6. It can be observed that the radiation pattern tends to deflect to the left (right) when d_1 decreases (increases). Thus, the d_1 can be used to adjust the symmetry of the radiation pattern. If the MTS SET I are placed symmetrically along y-direction with respect to x-axis, the radiation pattern would deflect to left. Therefore, in order to realize a symmetrical dual-beam pattern, the left and right side arrays are placed asymmetrically with $d_1 = 5.3$ mm and $d_2 = 4.3$ mm.

To better exemplify the effect of dual-beam generation, the electric field distributions of four antennas depicated in Fig. 4 on the XY plane at 26 GHz are given in Fig. 7. Fig. 7(a) shows that the wave propagates to the end-fire direction for Antenna I. Fig. 7(b) displays that the beamwidth for Antenna II is broadened by adding MTM SET I compared with Antenna I. Besides, after loading MTM SET II, the dual beam can be created, as shown in Fig. 7(c). The dual beam for antenna IV illustrated in Fig. 7(d) is further enhanced by incorporating MTM SET III.

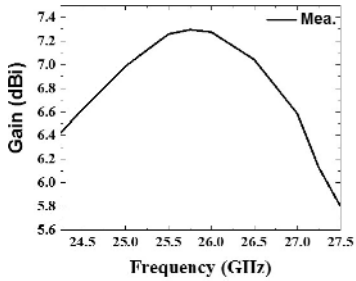

Fig. 10. The gain versus the frequency at radiation direction of 30°.

To validate the proposed method, a photograph of the proposed antenna IV is fabricated, the photo of which is illustrated in Fig. 8(a). The reflection coefficient is measured by the Agilent PNX-X-N5245A vector network analyzer, and the measured and simulated results are plotted in Fig. 8(b). It can be observed that the measured result agrees very well with simulated one except for a slight frequency shift of less than 1%, which may be caused by the fabrication and assembly errors.

The radiation patterns and gain of the proposed antenna are measured in an anechoic chamber as shown in Fig. 9(a). The measured and simulated E-plane radiation patterns of the proposed antenna at 25, 26, and 27 GHz are shown in Fig. 9(b)–(d), respectively. The measured radiation patterns match very well with the simulated ones. The measured results indicate that dual-beam can be realized over the operating band with the main beam radiating to $\pm 30^\circ$ with respect to the end-fire direction. The gains are 7.1, 7.4, and 6.6 dBi at 25, 26, and 27 GHz, respectively, while the corresponding radiation nulls are -9.2,-17.6, and -10.1 dBi, respectively. Because the gain varying with frequency at radiation direction of -30° is almost the same as that of 30°. Fig. 10 only plots the measured gain versus frequency at the radiation direction of 30°. It can be observed that the maximum gain is 7.4 dBi at 26 GHz.

4. Conclusions

In this work, a technique to generate a symmetrical dual-beam planar end-fire bowtie antenna in E-plane with gain enhancement is demonstrated, which can be obtained by integrating HRI medium in front of the bowtie antenna. The HRI medium can be realized by using triple-I-type MTM arrays. A pair of HRI MTM arrays are seated side by side to the radiators in order to form a wide beam antenna. Then,another pair of HRI MTM arrays are deliberated to place asymmetrically along y-direction regarding to x-axis in order to achieve a symmetrical dual-beam radiation pattern. An anisotropic unit cell with respectively HRI and near zero refractive index in x- and y-directions is proposed and designed to further improve the directivity. The measured results agree well with simulated one. The measured results reveal that the symmetrical dual-beam planar bowtie antenna in E-plane can be obtained at $\pm 30^\circ$ with respect to the end-fire direction over 24.25–27.5 GHz with good impedance matching. The maximum gain reaches 7.4 dBi at 26 GHz, which improves 4.2 dB compered to the wide beam antenna. The radiation null in the end-fire direction is -17.6 dB. The proposed antenna features low fabrication cost and low complexity. Therefore, it is an attractive alternative for 5G MIMO application at high frequency.

References

[1] A. L. Swindlehurst, E. Ayanoglu, P. Heydari, and F. Capolino, “Millimeter-wave massive MIMO: The next wireless revolution?” *IEEE Commun. Mag.*, vol. 52, no. 9, pp. 56–62, Sep. 2014.

[2] A. I. Sulyman, A. T. Nassar, M. K. Samimi, G. R. Maccartney, T. S. Rappaport, and A. Alsanie, “Radio propagation path loss models for 5G cellular networks in the 28 GHZ and 38 GHZ millimeter-wave bands,” *IEEE Commun. Mag.*, vol. 52, no. 9, pp. 78–86, Sep. 2014.

[3] A. Gupta and R. K. Jha, "A survey of 5G network: Architecture and emerging technologies," *IEEE Access*, vol. 3, pp. 1206–1232, 2015.
[4] R. Waterhouse and D. Novack, "Realizing 5G: Microwave photonics for 5G mobile wireless systems," *IEEE Microw. Mag.*, vol. 16, no. 8, pp. 84–92, Sep. 2015.
[5] H. Jin, W. Che, K. Chin, G. Shen, W. Yang, and Q. Xue, "60-GHz LTCC differential-fed patch antenna array with high gain by using soft-surface structures," *IEEE Trans. Antennas Propag.*, vol. 65, no. 1, pp. 206–216, Jan. 2017.
[6] O. Yurduseven and D. R. Smith, "Dual-polarization printed holographic multibeam metasurface antenna," *IEEE Antennas Wireless Propag. Lett.*, vol. 16, pp. 2738–2741, 2017.
[7] X. Cheng *et al.* "A compact multi-beam end-fire circularly polarized septum antenna array for millimeter-wave applications," *IEEE Access*, vol. 6, pp. 62784–62792, 2018.
[8] K. Sang-Gyu and C. Kai, "Independently controllable dual-feed dual-beam phased array using piezoelectric transducers," *IEEE Antennas Wireless Propag. Lett.*, vol. 1, pp. 81–83, 2002.
[9] S. Kirthiga and M. Jayakumar, "Performance of dualbeam MIMO for millimeter wave indoor communication systems," *Wireless Pers. Commun.*, vol. 77, no. 1, pp. 289–307, 2014.
[10] T. L. Chen and Y. D. Lin, "Dual-beam microstrip leaky-wave array excited by aperture-coupling method," *IEEE Trans. Antennas Propag.*, vol. 51, no. 9, pp. 2496–2498, Sep. 2003.
[11] Z. L. Ma and L. J. Jiang, "One-dimensional triple periodic dual-beam microstrip leaky-wave antenna," *IEEE Antennas Wireless Propag. Lett.*, vol. 14, pp. 390–393, 2015.
[12] A. Khidre, K. F. Lee, A. Z. Elsherbeni, and F. Yang, "Wide band dual-beam U-slot microstrip antenna," *IEEE Trans. Antennas Propag.*, vol. 61, no. 3, pp. 1415–1418, Mar. 2013.
[13] Y. G. Ma, P. Wang, X. Chen, and C. K. Ong, "Near-field plane-wave-like beam emitting antenna fabricated by anisotropic metamaterial," *Appl. Phys. Lett.*, vol. 94, no. 4, 2009, Art. no. 044107.
[14] Q. Cheng, W. X. Jiang, and T. J. Cui, "Radiation of planar electromagnetic waves by a line source in anisotropic metamaterials," *J. Phys. D-Appl. Phys.*, vol. 43, no. 33, 2010, Art. no. 335406.
[15] B. Zhou and T. J. Cui, "Directivity enhancement to Vivaldi antennas using compactly anisotropic zero-index metamaterials," *IEEE Antennas Wireless Propag. Lett.*, vol. 10, pp. 326–329, 2011.
[16] N. Wang, H. Chen, W. Lu, S. Liu, and Z. Lin, "Giant omnidirectional radiation enhancement via radially anisotropic zero-index metamaterial," *Opt. Express*, vol. 21, no. 20, pp. 23712–23723, 2013.
[17] C. Zhou, S. W. Cheung, Q. Li, and M. Li, "Bandwidth and gain improvement of a crossed slot antenna with metasurface," *Appl. Phys. Lett.*, vol. 110, no. 21, 2017, Art. no. 211603.
[18] S. Wu, Y. Yi, Z. Yu, X. Huang, and H. Yang, "A zero-index metamaterial for gain and directivity enhancement of tapered slot antenna," *J. Electromagn. Waves Appl.*, vol. 30, no. 15, pp. 1993–2002, 2016.
[19] M. Bhaskar, E. Johari, Z. Akhter, and M. J. Akhtar, "Gain enhancement of the Vivaldi antenna with band notch characteristics using zero-index metamaterial," *Microw. Opt. Techn. Lett.*, vol. 58, no. 1, pp. 233–238, 2016.
[20] L. Si, W. Zhu, and H. Sun, "A compact, planar, and CPW-fed metamaterial-inspired dual-band antenna," *IEEE Antennas Wireless Propag. Lett.*, vol. 12, pp. 305–308, 2015.
[21] L. Si *et al.* "A uniplanar triple-band dipole antenna using complementary capacitively loaded loop," *IEEE Antennas Wireless Propag. Lett.*, vol. 14, pp. 743–746, 2015.
[22] A. Dadgarpour, B. Zarghooni, B. S. Virdee, and T. A. Denidni, "Beam tilting antenna using integrated metamaterial loading," *IEEE Trans. Antennas Propag.*, vol. 62, no. 5, pp. 2874–2879, May 2014.
[23] A. Dadgarpour, B. Zarghooni, B. S. Virdee, and T. A. Denidni, "Single end-fire antenna for dual-beam and broad beamwidth operation at 60 GHz by artificially modifying the permittivity of the antenna substrate," *IEEE Trans. Antennas Propag.*, vol. 64, no. 9, pp. 4068–4073, Sep. 2016.
[24] J. Li, Q. Zeng, R. Liu, and T. A. Denidni, "Beam-tilting antenna with negative refractive index metamaterial loading," *IEEE Antennas Wireless Propag. Lett.*, vol. 16, pp. 2030–2033, 2017.
[25] A. Dadgarpour, M. S. Sorkherizi, A. A. Kishk, and T. A. Denidni, "Single-element antenna loaded with artificial mu-near-zero structure for 60 GHz MIMO applications," *IEEE Trans. Antennas Propag.*, vol. 64, no. 12, pp. 5012–5019, Dec. 2016.
[26] A. Dadgarpour, M. S. Sorkherizi, T. A. Denidni, and A. A. Kishk, "Passive beam switching and dual-beam radiation slot antenna loaded with ENZ medium and excited through ridge gap waveguide at millimeter-waves," *IEEE Trans. Antennas Propag.*, vol. 65, no. 1, pp. 92–102, Jan. 2017.
[27] Y. Huang, L. Yang, J. Li, Y. Wang, and G. Wen, "Polarization conversion of metasurface for the application of wide band low-profile circular polarization slot antenna," *Appl. Phys. Lett.*, vol. 109, no. 5, 2016, Art. no. 054101.
[28] H. Xu *et al.*, "Chirality assisted high efficiency metasurfaces with independent control of phase, amplitude, and polarization," *Adv. Opt. Mater.*, vol. 6, 2018, Art. no. 1801479.
[29] R. Liu, C. Ji, J. J. Mock, J. Y. Chin, T. J. Cui, and D. R. Smith, "Broadband ground-plane cloak," *Science*, vol. 323, pp. 366–369, 2009, Art. no. 5912.
[30] D. R. Smith, D. C. Vier, T. Koschny, and C. M. Soukoulis, "Electromagnetic parameter retrieval from inhomogeneous metamaterials," *Phys. Rev. E*, vol. 71, no. 6, 2005, Art. no. 036609.
[31] S. Microwave. 1.85 mm connectors. [Online]. Available: http://www.southwestmicrowave.com/